



Title	Adherence of Fine Wires : Solution by Energy Minimum Principle and Nano Adhesional Bonding(Physics, Processes, Instruments & Measurements)
Author(s)	Takahashi, Yasuo
Citation	Transactions of JWRI. 2001, 30(2), p. 23-31
Version Type	VoR
URL	https://doi.org/10.18910/3971
rights	
Note	

The University of Osaka Institutional Knowledge Archive : OUKA

<https://ir.library.osaka-u.ac.jp/>

The University of Osaka

Adherence of Fine Wires ---Solution by Energy Minimum Principle and Nano Adhesional Bonding ---†

Yasuo TAKAHASHI*

Abstract

Surface activated adhesional elastic contact solution between cylindrical bodies (wires) is deduced by energy minimum principle. The energy difference of $\Delta\gamma = 2\gamma_s - \gamma_i$ makes the contact width greater than Hertz's solution, where γ_s is the surface energy and γ_i is the interface energy at the contact area. The adhesional contact width a_j is given by

$$f = \frac{R}{4R_1 R_2 k} \cdot a_j^2 - \left(\frac{\Delta\gamma}{k} \cdot a_j \right)^{\frac{1}{2}},$$

where k is expressed by $k = (k_1 + k_2)/2$. Here, k_1 and k_2 are the elastic constants of two cylindrical bodies (or fine wires), R_1 and R_2 are the radii of two cylinders, $R = (R_1 + R_2)/2$, and f is the applied force per unit length of cylinders.

The adhesional elastic contact width a_j without load ($f = 0$) is given by

$$a_j = \alpha \cdot R^{2/3} \cdot (k \cdot \Delta\gamma)^{1/3},$$

where α is the constant and $\alpha = 4^{2/3}$ for wire-wire contact with a same radius, $\alpha = 4$ for wire-plane contact and $\alpha = 4^{5/6}$ for wire-rigid plane contact. The contact ratio a_j/R increases as R decreases, because $a_j/R \propto R^{-1/3}$. It is suggested that heatless and pressureless nano-order interconnection is possible.

Also, the possibility of nano adhesional bonding of very fine Au wire is discussed, taking into account some calculated results. Futher, an experimental evidence of Au wire adhesional bonding is shown.

KEY WORDS: (Adherence) (Adhesion) (Surface energy) (Fine wire) (Room temperature) (Adhesional contact) (Nano bonding) (Elastic contact)

1. Introduction

As the two bodies to be bonded becomes smaller, the cohesive force (adherence) becomes large, because the effect of surface energy becomes strong. For example, if the surfaces are activated by Ar ion bombardment under ultra high vacuum conditions ($< 1.3 \times 10^{-7}$ Pa), the surface energy γ_s increases. This implies that nano adhesional bonding without the bonding pressure is possible. It is interesting to theoretically realize the size of bodies which begins to produce the adhesional bonding.

The contact area (and/or radius) and the adhesive force between a small sphere body and a flat plane were first formulated by Johnson, Kendall and Roberts¹⁾, using the energy minimum principle (vertical work). Also, Takahashi and Onzawa^{2, 3)} took into account the effect of stiffness of the measurement system and the surface/surface interaction between contacted solid bodies and confirmed the neces-

sity and usefulness of the energy minimum method and the continuum approximation for systematically understanding the adhesional contact.

However, because of the difficulties with respect to the plane strain displacements, nobody has deduced the adhesional contact formulation between cylindrical bodies, based on the energy minimum principle(strain energy release). On the other hand, Barquins^{4, 5)} found another method to deduce the theoretical adhesional contact by introducing the idea of Griffith's criterion and the stress intensity factor and applied it for calculating the contact between a rigid cylinder and a flat surface⁵⁾. This method is valid for the case when there are no effects of stiffness of the measurement system and an attractive effect of surface. The energy minimum principle is useful for the case when various effects exist. In other words, the energy minimum vertical work principle is a genenal solving method for any problem. Also,

† Received on November 7, 2001

* Associate professor, JWRI, Osaka University

Transactions of JWRI is published by Joining and Welding Research Institute of Osaka University, Ibaraki, Osaka 567-0047, Japan.

even if one is not familiar with fracture mechanics and the idea of Griffith's criterion and the stress intensity factor, he can calculate the adhesional contact width, using the energy minimum principle. Barquin's method is too simple for one who is not familiar with the fracture mechanics to understand the physical meaning. On the other hand, the method based on the energy minimum principle gives the physical meaning understandable to anybody although it is very troublesome. The solving process based on the energy minimum principle will be helpful to find the solution for the adhesional contact problems together with other effects.

The formula for the adhesional elastic contact between cylindrical bodies was necessary for the author to study the micro or nano adhesional bonding between fine gold wire and flat gold pad (plate or foil) because the formula gives the theoretical pull strength and contact area (width). Therefore, the purpose of the present paper is to find the adhesional elastic contact width for any cylindrical bodies, based on the strain energy minimum principle. The author expects that this solving process will be helpful for the solution of the adhesional contact affecting another external effect. Also, the possibility of nano adhesional bonding and its problems will be discussed, taking some calculated and experimental results into consideration.

2. Hertz's Solution

More than one century has passed since Hertz proposed the contact theory between two elastic bodies^{6,7)} but his theory is now very helpful to deduce the solution of adhesional contact of cylindrical bodies. At first, Hertz's solution is summarized here.

The situation when the two cylindrical bodies are contacted parallel to each other is illustrated in **Fig. 1**, where R_1 and R_2 are the radii of cylinders (wires). If the force F (= f) is applied to a unit length of the cylinders, then half the elastic contact width a of Hertz's solution is given

$$a = \left\{ \frac{4R_1R_2}{R_1 + R_2} (k_1 + k_2) f \right\}^{\frac{1}{2}}, \quad (1)$$

where k_1 and k_2 are elastic constants and they are expressed by

$$k_1 = \frac{1 - \nu_1^2}{E_1} \quad \text{and} \quad k_2 = \frac{1 - \nu_2^2}{E_2},$$

respectively. Also, ν is a Poisson's ratio and E is Young's modulus of the cylinders and the subscripts 1 and 2 denote the distinction of two cylinders.

The compressive stress distribution σ_h on the contact inter-

face in the x direction is given by

$$\begin{aligned} \sigma_h &= \frac{1}{\pi} \sqrt{\left\{ \frac{(R_1 + R_2) \cdot f}{R_1 R_2 (k_1 + k_2)} \right\} \left(1 - \frac{x^2}{a^2} \right)} \\ &= p_o \sqrt{1 - \frac{x^2}{a^2}}, \end{aligned} \quad (2)$$

where p_o is expressed by

$$p_o = \frac{2f}{\pi a}.$$

3. Compression amount of cylinders

The compression amount (approach distance) δ of two elastic cylinders is necessary to calculate the adhesional contact width a , based on the energy minimum principle.

In two wires contacted as shown in **Fig. 1**, the stress components, σ_x and σ_z along the z axis are, respectively, expressed by

$$\sigma_x = -p_o \left\{ \frac{a^2 + 2z^2}{a\sqrt{z^2 + a^2}} - \frac{2z}{a} \right\} \quad (3)$$

and

$$\sigma_z = -p_o \cdot \frac{a}{\sqrt{z^2 + a^2}}, \quad (4)$$

where the tensile stress takes a plus sign.

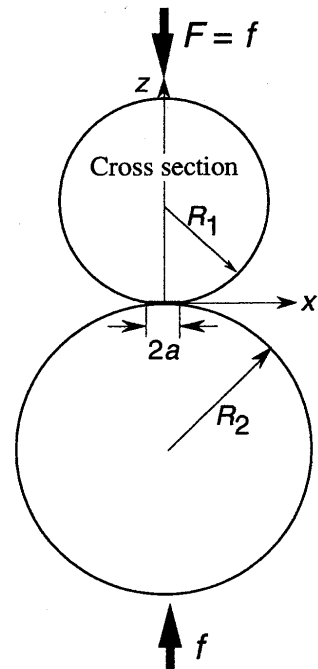


Fig. 1 Schematic illustration of two cylindrical bodies in contact (cross section).

Because of plane strain condition, i.e., the strain in the y direction (the longitudinal direction of cylinders) can be neglected ($\epsilon_y = 0$), $\sigma_y = \nu(\sigma_x + \sigma_z)$ holds good. The principal strain in the z direction is, therefore, obtained as

$$\begin{aligned}\epsilon_z &= \frac{1}{E} \{ \sigma_z - \nu(\sigma_x + \sigma_y) \} \\ &= \pi k \left(\sigma_z - \frac{\nu}{1-\nu} \sigma_x \right) \quad (5)\end{aligned}$$

where k is expressed by

$$k = \frac{1-\nu^2}{\pi E}.$$

As the whole displacement w_1 in the z direction of cylinder 1 is solved from

$$w_1 = \int_0^{2R_1} \epsilon_z dz,$$

after eqs. (3) and (4) is substituted into eq. (5), w_1 is obtained by

$$\begin{aligned}w_1 &= 2k_1 f \left[\ln \frac{a}{\sqrt{4R_1^2 + a^2 + 2R_1}} \right] \\ &+ 2k_1 f \left[\frac{\nu_1}{1-\nu_1} \left\{ \frac{1}{4a^2} \left(\sqrt{4R_1^2 + a^2} + 2R_1 \right)^2 \right\} \right] \\ &- 2k_1 f \left[\frac{\nu_1}{1-\nu_1} \left\{ \frac{a^2}{4} \cdot \left(\sqrt{4R_1^2 + a^2} + 2R_1 \right)^{-2} + \frac{4R_1^2}{a^2} \right\} \right]. \quad (6)\end{aligned}$$

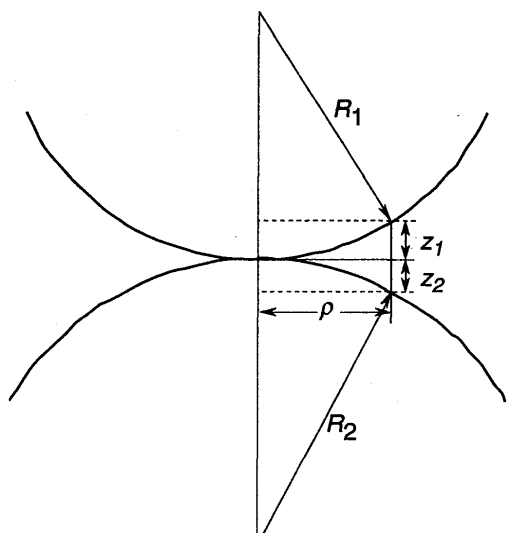


Fig. 2 Schematic illustration of elastic contact zone of cylindrical bodies (wires) and definition of parameters z_1 , z_2 , and ρ .

Because R_1 is usually much greater than the contact width $2a$, eq. (6) can be approximated to

$$w_1 = 2k_1 f \ln \frac{4R_1}{a}. \quad (7)$$

In the same manner, the displacement w_2 for cylinder 2 is obtained by

$$w_2 = 2k_2 f \ln \frac{4R_2}{a}. \quad (8)$$

The integration of eq. (5) makes the displacements w_1 and w_2 less than zero but the eqs. (7) and (8) are made greater than zero by taking a plus sign for the compression.

In Fig. 2, z_1 and z_2 are given by

$$z_1 \approx \frac{\rho}{2R_1} \quad \text{and} \quad z_2 \approx \frac{\rho}{2R_2},$$

respectively⁷⁾. The total approach distance δ is, therefore, obtained by

$$\begin{aligned}\delta &= (w_1 + w_2) + (z_1 + z_2) \\ &= w_1 + w_2 + \frac{\rho^2}{2} \left(\frac{1}{R_1} + \frac{1}{R_2} \right), \quad (9)\end{aligned}$$

where ρ can be defined as

$$\rho = a / \sqrt{2},$$

because δ and $\partial\delta/\partial f$ should be always greater than zero as stated below (this definition of ρ can be understood in Appendix). If $\delta < 0$, the wires are extended in the z direction by the compressive force f . Thus, the total approach distance δ is expressed by

$$\delta = 2k f \left(\frac{k_1}{k} \ln \frac{4R_1}{a} + \frac{k_2}{k} \ln \frac{4R_2}{a} + 1 \right), \quad (10)$$

where k is redefined as

$$k = \frac{k_1 + k_2}{2}. \quad (11)$$

After substituting a of eq. (1) into a in eq. (10),

$$\delta = 2k f (g+1) \quad (12)$$

is obtained, where g is given by

$$g = \frac{k_1}{2k} \ln \left(\frac{4R}{kf} \cdot \frac{R_1}{R_2} \right) + \frac{k_2}{2k} \ln \left(\frac{4R}{kf} \cdot \frac{R_2}{R_1} \right), \quad (13)$$

where R is expressed by

$$R = \frac{R_1 + R_2}{2}. \quad (14)$$

The differential of eq. (10) with respect to the force f is

$$\frac{d\delta}{df} = 2kg, \quad (15)$$

because $g' = dg/df = -1/f$. Equations (10), (13) and (15) are necessary for solving the adhesional contact width $2a_j$ for cylindrical bodies.

4. Energy balance in adhesional contact (energy minimum principle)

The difference between the surface energy and the contacted interface energy $\Delta\gamma (= \gamma_{s1} + \gamma_{s2} - \gamma_i)$ has an influence on the contact behavior of two solid bodies as the applied compressive force f decreases¹⁾. Here, γ_{s1} and γ_{s2} are the surface energies of cylinders (wires) 1 and 2, respectively, and also γ_i is the interface energy of the contact zone. If $\Delta\gamma = 0$, the contact width a is given by eq.(1), and also the stress distribution σ_h is obtained by eq. (2).

On the other hand, when $\Delta\gamma > 0$, the adhesional contact width a_j is greater than Hertz's solution a_h . In other words, there is a situation where $a_j (f = f_j)$ is equal to $a_h (f = f_h)$, under the condition of f_j less than f_h . Here, f_h is the applied compressive force to obtain the elastic contact a without $\Delta\gamma$.

Boussinesq's stress distribution σ_m needs to be introduced in order to consider the force reduction $|f_h - f_j|$. Boussinesq's stress distribution along the x axis for the applied force F is expressed by

$$\sigma_m = \frac{F}{\pi \cdot \sqrt{a^2 - x^2}} = \frac{f_j - f_h}{\pi \cdot \sqrt{a^2 - x^2}}. \quad (16)$$

Muskhelishvili's stress distribution can take the place of Boussinesq's stress distribution because they are essentially equal to each other.

Fig. 3 illustrates Boussinesq's stress distribution for $F = f_j - f_h$, together with the stress distributions σ_h and σ_j , where a negative value is taken for the compressive stress,

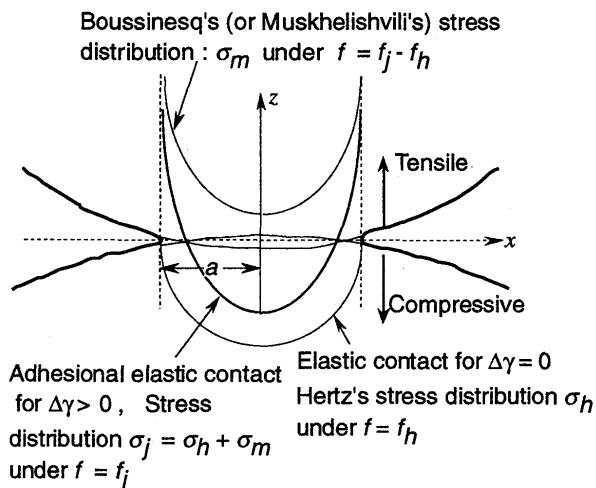


Fig. 3 Schematic illustration of stress distribution in the contact area.

i.e., $f_j < 0$ and $f_h < 0$, and $(f_j - f_h) > 0$ are assumed in Fig. 3. From Boussinesq's relation²⁾, the stress distribution σ_j for the adhesional contact can be obtained by $\sigma_j = \sigma_h + \sigma_m$.

The force reduction of $|f_h - f_j|$ does not break the contact area because of $\Delta\gamma$, i.e., $a_j = a_h$ is kept even under $f = f_j$ ($|f_j| < |f_h|$) and the stress distribution σ_j remains as a residual stress. Thus, there exists an energy balance between the elastic stress field and $\Delta\gamma$. This means that an energy minimum situation is established.

The stored energy due to the elastic contact is equal to the integration of f by δ , taking a plus sign for the compression.

Fig. 4 illustrates the relation between δ and f . The curve OA is for Hertz contact, obtained by eq. (12). The contact width a_h is attained at the point A ($f = f_h$, $\delta = \delta_h$). Because of Boussinesq's relation²⁾, the force reduction occurs along the tangential line of the curve OA at the point A, keeping $a = a_h$. The straight line AB is expressed by

$$\begin{aligned} (\delta - \delta_h) &= \left[\frac{d\delta}{df} \right]_{f_h} \cdot (f - f_h) \\ &= 2kg_h \cdot (f - f_h), \end{aligned} \quad (17)$$

where $[d\delta/df]_{f_h}$ is the slope of the tangential line AB at $f = f_h$ and also δ_h and δ_j are, respectively, defined as $\delta(f_h)$ and $\delta(f_j)$ from eq. (12) and g_h is given by $g_h = g(f_h)$ from eq. (13).

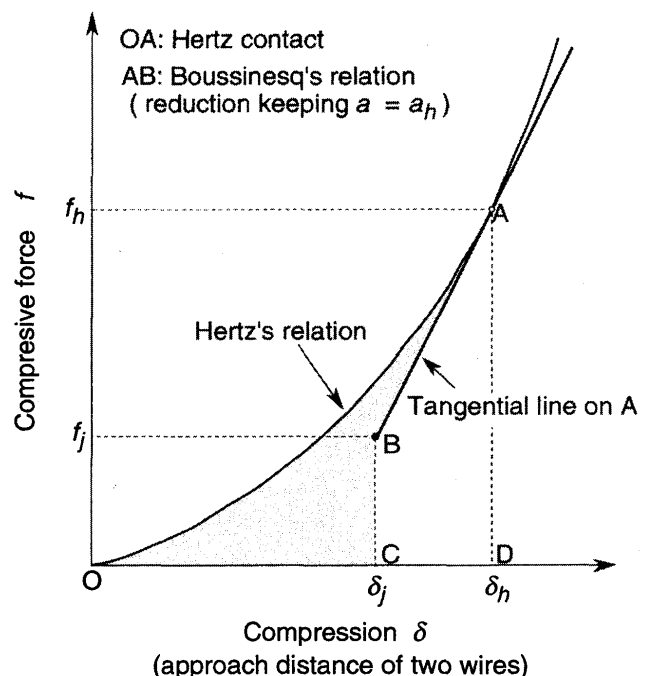


Fig. 4 Relation between force and approach distance. The curve OA is given by Hertz's relation and the tangential line is Boussinesq's relation.

The elastic energy ABCD is released due to the force reduction. As a result, the elastic energy OABC (gray area) remains. It is geometrically understood that the stored elastic energy OABC is expressed by

$$E_{elastic} = E_1 - E_2 - E_3, \quad (18)$$

where E_1 is the Rectangle of ODA f_h , E_2 is the area ABCD and E_3 is the area OA f_h . E_1 , E_2 , and E_3 are, respectively, given by

$$E_1 = f_h \cdot \delta_h, \quad (19)$$

$$E_2 = \frac{1}{2}(\delta_h - \delta_j)(f_j + f_h), \quad (20)$$

and

$$E_3 = \int_0^{f_h} \delta(f) df. \quad (21)$$

The adhesional contact due to the surface energy loss $\Delta\gamma$ is established at the point B. Thus, the total energy remaining at the point B is given by

$$E_{total} = E_{elastic} - E_4, \quad (22)$$

where E_4 is expressed by $E_4 = 2a_h \cdot \Delta\gamma$ as a value per unit length of cylinders. We can calculate $a = a_h$ under the condition of $f = f_j$ (at the point B of $\delta = \delta_j$) by the principle of energy minimum, i.e., this means to calculate a_h (or f_h for the solution a_h) by making E_{total} minimum under the condition of $\delta = \delta_j$ (or $f = f_j$), that is, the solution is obtained when

$$\left[\frac{\partial E_{total}}{\partial a_h} \right]_{\delta=\delta_j} = \frac{\partial E_{total}}{\partial f_h} \cdot \frac{f_h}{a_h} = 0 \quad (23)$$

is satisfied, i.e., $\partial E_{total} / \partial f_h = 0$.

5. Effective contacting force

The effective contacting force f_e ($= f_h$) can be calculated as a function of f_j from

$\partial E_{total} / \partial f_h = 0$. From eq. (A-7) in Appendix,

$$(\delta_h - \delta_j)^2 = 2^3 \cdot g_h^2 \cdot \Delta\gamma \left(\frac{R_1 R_2 \cdot k^3}{R} f_h \right)^{\frac{1}{2}} \quad (24)$$

is obtained. Because of $g_h > 0$ (see Appendix),

$$\delta_h - \delta_j = 2^{3/2} \cdot g_h \cdot \Delta\gamma^{\frac{1}{2}} \cdot \left(\frac{R_1 R_2 \cdot k^3}{R} f_h \right)^{\frac{1}{4}} \quad (25)$$

is established. After substituting eq. (25) into eq. (A-1) in Appendix to eliminate g_h ,

$$f_j = f_h - 2 \cdot \left\{ \frac{R_1 R_2}{R_1 + R_2} \cdot \frac{1}{k_1 + k_2} f_h \right\}^{\frac{1}{4}} \cdot \Delta\gamma^{\frac{1}{2}} \quad (26)$$

is obtained. Eq. (26) shows that f_j is expressed as a function only of f_h . In eq. (26), if f_j and f_h are replaced by f and f_e , respectively, f_e is the effective force to give the adhesional contact width a_j under the applied force f .

Fig. 5 shows the relation between f_e and f , taking a positive sign for compression force. The material constants used in the present study are shown in Table 1.

It is easy to understand that df_e / df (or df / df_e) ≥ 0 , if taking a plus sign for the compression, i.e., f_e should not

Table 1 Material constants of pure gold.

Name	Symbol	Value (Unit)
Surface energy	γ_s	$1.485 \text{ (J m}^{-2}\text{)}$
Interface energy	γ_i	$0.36 \text{ (J m}^{-2}\text{)}$
Energy difference	$\Delta\gamma = 2\gamma_s - \gamma_i$	$2.61 \text{ (J m}^{-2}\text{)}$
Shear modulus at 300K	$G(300)$	$2.91 \times 10^{10} \text{ (Nm}^{-2}\text{)}$
Poisson's ratio	ν	0.42
Young's modulus	$E = 2(1+\nu) G$	$8.27 \times 10^{10} \text{ (Nm}^{-2}\text{)}$
Elastic constant	k	$3.17 \times 10^{-12} \text{ (m}^2\text{N}^{-1}\text{)}$
Yield stress at 300K for annealed gold	σ_y	$9.93 \times 10^7 \text{ (Nm}^{-2}\text{)}$

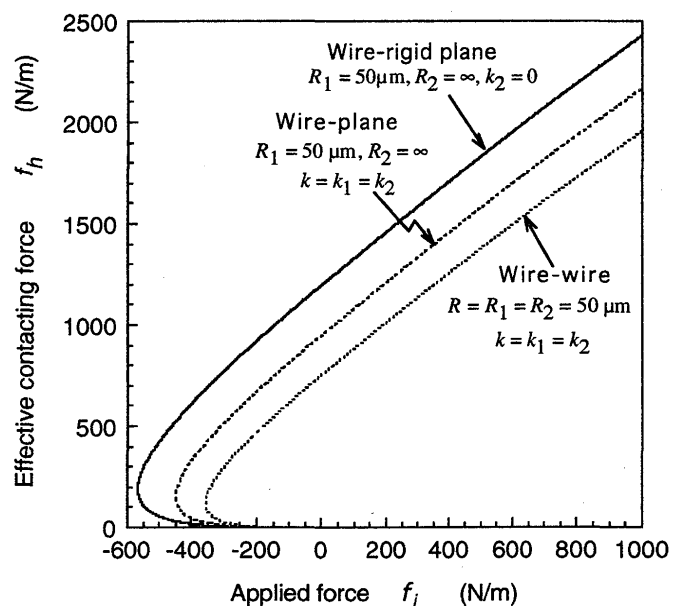


Fig. 5 Relation between effective force and applied force. The effective force f_e is obtained as f_h in eq. (26) for each applied force f ($= f_j$).

Adherence of Fine Wires

decreases as f increases as seen in Fig. 5. Therefore,

$$f_e \geq \left(\frac{K}{2}\right)^{\frac{4}{3}} \quad (27)$$

has to be established, where K is expressed by

$$K = \left\{ \frac{R_1 R_2}{R_1 + R_2} \cdot \frac{1}{k_1 + k_2} \right\}^{\frac{1}{4}} \cdot \Delta\gamma^{\frac{1}{2}}. \quad (28)$$

The effective force f_e ($= f_h$) and the applied force f_j show the one-to-one correspondence under the condition of eq. (27). Therefore, when the applied force $f = f_j$ is given, the effective contacting force f_e is obtained from eq. (26). When $f_e = (K/2)^{4/3}$, the minimum applied force

$$f_{\min} = -3 \left(\frac{K}{2}\right)^{\frac{4}{3}} \quad (29)$$

is obtained, which gives the minimum adhesional contact width $2a_{j\min}$ as mentioned below.

The minimum applied force for spheres is independent of the elastic modulus[9]. On the other hand, the minimum applied force f_{\min} of cylinders depends on it.

6. Adhesional contact width

As stated above, the effective force f_e is easily calculated for each applied force $f = f_j$ in eq. (26). After f_e is substituted into f in eq. (1), half the contact width $a(f_e)$ is obtained. This corresponds to the adhesional contact width a_j under the applied force $f = f_j$. The adhesion does not occur under the condition of $f < f_{\min}$, i.e., f_{\min} is the force for separating two cylinders.

The minimum adhesional contact width $a_{j\min}$ for $f = f_{\min}$ is given by

$$a_{j\min} = \left(\frac{R_1 R_2}{R}\right)^{\frac{2}{3}} (k \cdot \Delta\gamma)^{1/3}. \quad (30)$$

From the above, the effective force f_e for a_j is obtained by

$$f = f_e - \left(\frac{4 R_1 R_2}{Rk} \cdot f_e\right)^{\frac{1}{4}} \cdot \Delta\gamma^{\frac{1}{2}} \quad (31)$$

and the adhesional contact width is given by

$$a_j = \sqrt{\frac{4 R_1 R_2}{R} k f_e}, \quad (32)$$

where $R = (R_1 + R_2)/2$ and $k = (k_1 + k_2)/2$. After eq. (32) is substituted into eq. (31), the relationship of a_j and f is ob-

tained as

$$f = \frac{R \cdot a_j^2}{4R_1 R_2 k} - \left(\frac{\Delta\gamma}{k} \cdot a_j\right)^{\frac{1}{2}}. \quad (33)$$

If $R_2 = \infty$ and $k_1 = 0$ in (33), the adhesional contact between the rigid cylinder and the elastic plane is obtained. This solution is perfectly equal to that of Barquins⁵⁾.

Fig. 6 shows the adhesional contact width a_j depending on the compressive force f , which is calculated by eq. (33). The radius R (or R_1) of Au wire is 50 μm . The applied mean

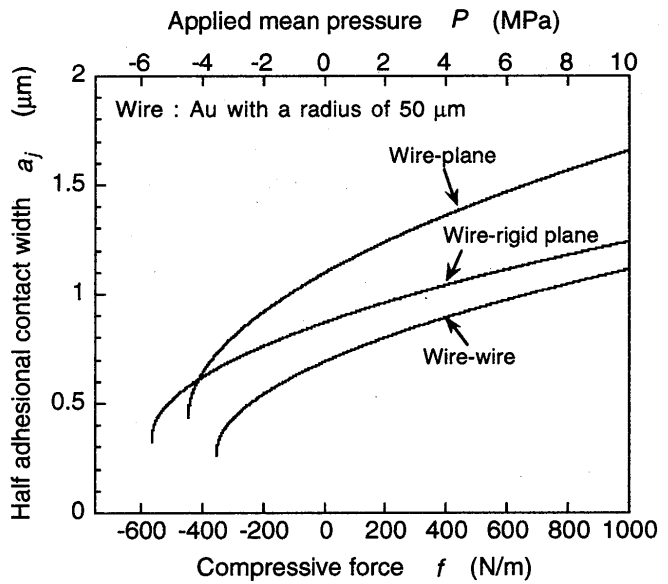


Fig. 6 Half the adhesional contact width a_j between cylindrical bodies. The adhesional contact width for wire/wire contact is different from that of wire-rigid plane contact.

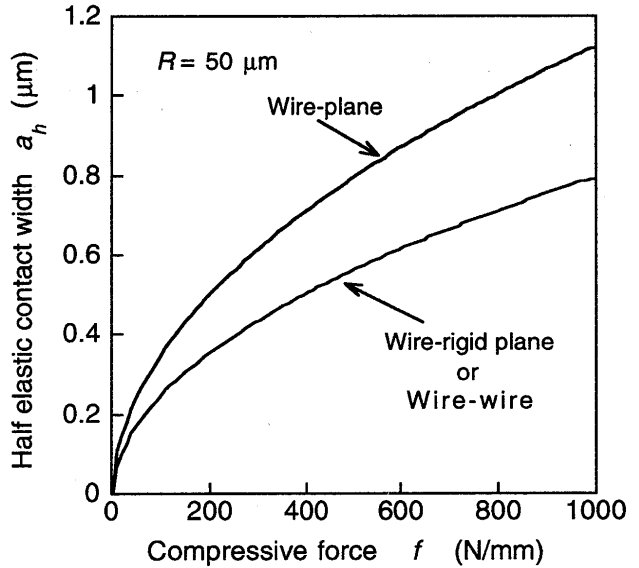


Fig. 7 Elastic contact of cylindrical bodies (Hertz's solution), calculated by eq. (1).

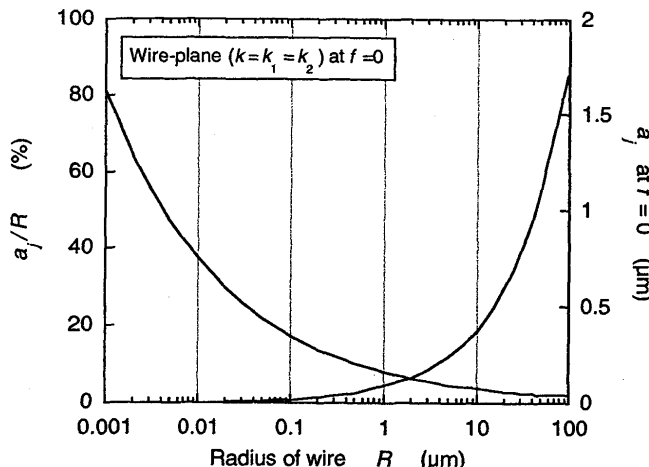


Fig. 8 Dependence of adhesional elastic contact width a_j for $f = 0$ N/m on wire radius R . The ratio of a_j/R increases as R decreases.

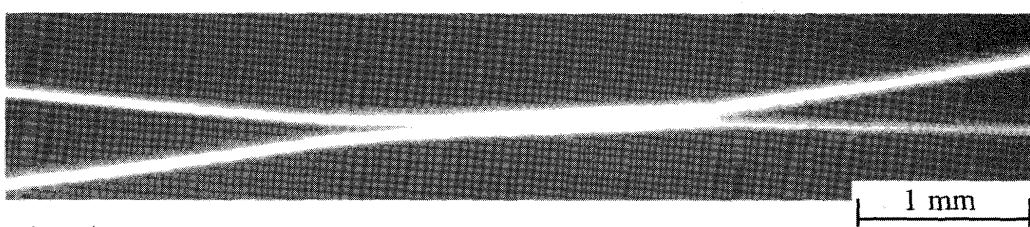
pressure P shown in the upper side of the figure is given by $P = f/2R$. The adhesional contact widths of three cases (wire-wire; $R = R_1 = R_2$ and $k = k_1 = k_2$, wire-plane; $R_1 = R$, $R_2 = \infty$ and $k = k_1 = k_2$, and wire-rigid-plane; $R_1 = R$, $R_2 = \infty$ and $k_2 = 0$) are exhibited. The contact width of wire-wire is the smallest among the three cases, while wire-plane gives the largest contact area. The solutions for three cases are shown in Appendix, which makes it easy to understand the adhesional contact behavior.

The solution exists even for $f < 0$, which is different from Hertz's solution of Fig. 7 calculated by eq. (1). Also, the adhesional contact width of wire-wire is different from that of wire-rigid plane. On the other hand, Hertz's solution gives the same contact width for wire-wire and wire-rigid plane.

8. Possibility of nano adhesional bonding

Fig. 8 shows the radius-dependence of a_j/R and a_j (wire-plane contact) under the condition of $f = 0$ (see Appendix). As seen in Fig. 8, as the radius R decreases, i.e., wire becomes fine, the adhesional contact ratio a_j/R increases. Because the assumption of $a_j \ll R$ at eq. (10) cannot be established when $R < 0.01$, the calculated results are not exact in the region $R < 0.01$, but this suggests that the wire, the radius of which is in nano order, gives a very large adhesional contact ratio even without the applied force. the adhesional bonding of very fine bodies is easily produced if the surfaces are activated⁸⁾. Very often the room temperature sintering of very fine particles occurs naturally. This is an example of nano adhesional bonding.

Fig. 9 shows an experimental result of adhesional contact between Au fine wire and Au pad (foil with thickness of 130 μm). The contact was carried out under the vacuum condition of 1.0×10^{-8} Pa after the surfaces were activated by Ar ion bombardment (Accelerating voltage 2 kV, Emission current 1 mA, Irradiation time 2 hr). The contact condition was the apparent applied pressure $P = 5$ MPa ($f = 500$ N/m), the temperature $T = 298$ K, the time for applying the force $t = 60$ s. The theory of adhesional contact (Fig. 6) predicts $a_j = 1.42$ μm but the experimental contact width a is from 1.8 μm to 2 μm. Also, $a = 1.0 \sim 1.4$ μm was experimentally obtained under $P = 2$ MPa and this is nearly equal to the theoretical value. However, $P = 20$ MPa gave $a = 3.4 \sim 5.4$ μm. This value is obviously different from the theoretical value as shown in Table 2. Another mechanism



$R = 50$ μm, $P = 5$ MPa (500 N/m), $a \approx 1.8 \sim 2$ μm, $F_p \approx 28$ mN

Fig. 9 Photograph of Au wire contacted with Au thin plate.

Table 2 Comparison between experimental half-contact width a and theoretical value a_j .

Condition	$P = 2$ MPa	$P = 5$ MPa	$P = 20$ MPa
Theoretical	$a_j = 1.24$ μm	$a_j = 1.42$ μm	$a_j = 1.96$ μm
Experimental	$a = 1.0 \sim 1.4$ μm	$a = 1.8 \sim 2$ μm	$a = 3.4 \sim 5.4$ μm

affects the adhesional contact under high pressure and this mechanism may be plastic deformation. The analysis of elastic-plastic contact is necessary.

The theoretical adherence force (adhesional fracture strength) is predicted by eq. (29) and the value for Au wire of $R = 50 \mu\text{m}$ -Au plate is 449 N/m (see Fig. 6). However, the experimental pull strength is $F_p \approx 28 \text{ mN}$ which is correspondent to 28 N/m. The experimental value of pull strength is much less than the theoretical one. This is due to the surface roughed by Ar ion bombardment. There may remain many problems from the view of actual bonding.

9. Conclusive remarks

The adhesional contact of fine cylindrical bodies has been discussed. The adhesional elastic contact width for fine cylindrical bodies has theoretically been deduced based on the energy minimum principle. As wire radius R decreases to nano scale, the adhesional elastic contact can become very large. This implies that the adhesional bonding may be very useful for the interconnection technology to construct nano scale systems and integrations. Also, experimental results suggests that the contact width is greater than the theoretical value as the applied force f increases and the pull strength is very different from the theoretical adhesional fracture strength. More detailed investigation is necessary.

[Appendix]

From eq. (12), $(d\delta/df)$ at $f = f_h$ ($= \delta_h'$) $= 2kg_h$, because of $(\partial g/\partial f)$ at $f = f_h$ ($= g_h'$) $= -f_h^{-1}$. Also, because the point B (δ_j, f_j) in Fig. 4 is given by eq. (17),

$$f_j = \frac{\delta_j - \delta_h}{2kg_h} + f_h \quad (\text{A-1})$$

is obtained. Therefore, eq. (20) is changed into

$$E_2 = -\frac{1}{2}(\delta_h - \delta_j) \left(\frac{\delta_j - \delta_h}{2kg_h} + 2f_h \right). \quad (\text{A-2})$$

$$\frac{\partial E_1}{\partial f_h} = \delta_h + 2kf_h g_h, \quad (\text{A-3})$$

and

$$\frac{\partial E_2}{\partial f_h} = -\frac{g_h}{4kg_h^2} (\delta_h - \delta_j)^2 - 2kg_h f_h. \quad (\text{A-4})$$

$$\therefore \partial \delta_h / \partial f_h \equiv \delta_h' = 2kg_h.$$

Also, $\partial E_3 / \partial f_h = \delta_h$ is clearly established as indicated in eq. (21). From eq. (1), E_4 is rewritten by

$$E_4 = 2a_h \Delta\gamma = 2\Delta\gamma \sqrt{\frac{4R_1 R_2 k}{R} \cdot f_h}. \quad (\text{A-5})$$

$\partial E_4 / \partial f_h$ is given by

$$\frac{\partial E_4}{\partial f_h} = \Delta\gamma \sqrt{\frac{4R_1 R_2 k}{R} \cdot \frac{1}{f_h}}, \quad (\text{A-6})$$

where $R = \frac{R_1 + R_2}{2}$ and $k = \frac{k_1 + k_2}{2}$. Therefore, a differential equation of

$$\frac{\partial E_{\text{total}}}{\partial f_h} = -\frac{g_h}{4kg_h^2} (\delta_h - \delta_j)^2 - \Delta\gamma \left(\frac{4R_1 R_2 k}{R f_h} \right)^{\frac{1}{2}} = 0 \quad (\text{A-7})$$

is obtained, where $g_h' \equiv (\partial g_h / \partial f_h) = -f_h^{-1}$. Eq. (24) in the text is obtained from Eq.(A-7).

In addition, because R_1 and R_2 is always greater than a_h ,

$$\left(\frac{4R_1}{a_h} \right)^2 = \frac{4R_1 R}{R_2 k f_h} > 1$$

and

$$\left(\frac{4R_2}{a_h} \right)^2 = \frac{4R_2 R}{R_1 k f_h} > 1$$

is established. Therefore, from eq. (13), the function, $g_h = g(f_h)$, is always greater than zero. That is, δ and $\partial \delta / \partial f_h$ are both always greater than zero from eqs. (12) and (15). It is, therefore, sufficient to adopt $\rho = a / \sqrt{2}$ for eq. (9) in order to obtain eq. (A-7).

Finally, the solutions of three cases of adhesional contact (wire-wire, wire-rigid plane, and wire-plane) are shown below for easily understanding the adhesional bonding.

(i) Wire-wire ($k = k_1 = k_2, R = R_1 = R_2$)

$$f = f_e - \left\{ \frac{4Rf_e}{k} \right\}^{\frac{1}{4}} \cdot \sqrt{\Delta\gamma} \quad (\text{A-8})$$

$$a_j = \sqrt{4Rk f_e} \quad (\text{A-9})$$

(ii) Wire-plane ($k = k_1 = k_2, R = R_1, R_2 = \infty$)

$$f = f_e - \left\{ \frac{8Rf_e}{k} \right\}^{\frac{1}{4}} \cdot \sqrt{\Delta\gamma} \quad (\text{A-10})$$

$$a_j = \sqrt{8Rkf_e} \quad (A-11)$$

(iii) Wire-rigid plane ($k = k_1, k_2 = \infty, R = R_1, R_2 = \infty$)

$$f = f_e - \left\{ \frac{16Rf_e}{k} \right\}^{\frac{1}{4}} \cdot \sqrt{\Delta\gamma} \quad (A-12)$$

$$a_j = \sqrt{4Rkf_e} \quad (A-13)$$

Also, half the adhesional elastic contact width for $f=0$ is given by

$$a_{j, \text{for } f=0} = \alpha \cdot R^{2/3} \cdot (k \cdot \Delta\gamma)^{1/3}, \quad (A-14)$$

where α is the constant. The value of α is $4^{2/3}$ for the wire-wire contact, $\alpha=4$ for the wire-plane contact, and $\alpha=4^{5/6}$ for the wire-rigid plane contact.

References

- 1) K. L. Johnson, K. Kendall, and A. D. Roberts, "Surface Energy and the Contact of Elastic Solids," Proc. Roy. Soc. Vol. A 324 (1971) pp. 301-313
- 2) K. Takahashi and T. Onzawa, "Influence of the Stiffness of the Measurement System on the Elastic adhesional contact," J. Adhesion Sci, Technol., Vol. 9, No. 11 (1995) pp. 1451-1464.
- 3) K. Takahashi and T. Onzawa, "Effect of the Stiffness of the Measurement System on Adhesion force curves in the Elastic Continuum limit," J. Adhesion Sci, Technol., Vol. 9, No. 11 (1995) pp. 1451-1464.
- 4) D. Maugis and M. Barquins, "Fracture Mechanics and The Adherence of viscoelastic bodies," J. Phys. D Appl. Phys., Vol. 11 (1978) pp. 1989-2023.
- 5) M. Barquins, "Adherence and Rolling Kinetics of a Rigid Cylinder in Contact with a Natural Rubber Surface," J. Adhesion, Vol. 26 (1988) pp.1-12.
- 6) H. Hertz, Miscellaneous Papers, Macmillan, London (1895-1896) p. 146, pp.179-195.
- 7) K. Ono, Mechanics, 2nd Edition, Maruzen, Tokyo (1938) pp.570-585.
- 8) Y. Sasaki, A. Kohno, and M. Horino, "Semiconductor Joining Technology Using Ar Atom Bombardment," Proc. of 2nd Symposium on "Microjoining and Assembly Technology in Electronics (Mate' 96)", Yokohama, Feb. 1-2 (1996) pp. 5-10.